http://doi.org/10.35784/iapgos.5610 received: 24.11.2023 | revised: 13.02.2024 | accepted: 10.03.2024 | available online: 31.03.2024

QUALITY INDICATORS OF DETECTION OF SIDE RADIATION SIGNALS FROM MONITOR SCREENS BY A SPECIALIZED TECHNICAL MEANS OF ENEMY INTELLIGENCE

Dmytro Yevgrafov, Yurii Yaremchuk
Vinnytsia National Technical University, Vinnytsia, Ukraine

Abstract. *The problem of calculating the quality indicators of detection of side radiation signals from static images on the monitor screen by a specialized technical means of enemy intelligence is solved, which implements an asymptotically optimal compatible algorithm for detecting side radiation signals and estimating the duration of image immutability on the monitor screen. The reliability of the calculation results was confirmed by modeling detection processes in the Mathcad and Excel software environments.*

Keywords: side electromagnetic radiation and targeting, Neumann-Pearson criterion, probability of false alarm, probability of signal miss

WSKAŹNIKI JAKOŚCI DO WYKRYWANIA SYGNAŁÓW PROMIENIOWANIA BOCZNEGO Z EKRANÓW MONITORÓW PRZEZ WYSPECJALIZOWANE ŚRODKI TECHNICZNE WYWIADU WROGA

Streszczenie*. W artykule rozwiązano problem obliczania wskaźników jakości wykrywania sygnałów promieniowania bocznego ze statycznych obrazów na ekranie monitora przez wyspecjalizowany techniczny środek rozpoznania wroga, który implementuje asymptotycznie optymalny wspólny algorytm wykrywania sygnałów promieniowania bocznego i szacowania czasu trwania stabilności obrazu na ekranie monitora. Wiarygodność wyników obliczeń została potwierdzona poprzez modelowanie procesów detekcji w środowisku oprogramowania Mathcad i Excel.*

Słowa kluczowe: zakłócenia elektromagnetyczne i przesłuchy, kryterium Neumanna-Pearsona, prawdopodobieństwo fałszywego alarmu, prawdopodobieństwo braku sygnału

Introduction

In [9], the asymptotically optimal algorithm of side radiation signals (SR) from monitor screens using liquid-crystal structures (LCS) is synthesized, which is used in modern specialized technical means of enemy intelligence (STMEI). In the STMEI, the functionality of the likelihood ratio (FLR) is calculated, which for $T_a >> T_f$ amounts to:

$$L(T_a) = \frac{4}{N_0 T_a}\sum_{k=1}^{K}\left[\left(\int_0^{T_a} x(t)\cos\left(\frac{2\pi kt}{T_f}\right)\mathrm{d}t\right)^2 + \left(\int_0^{T_a} x(t)\sin\left(\frac{2\pi kt}{T_f}\right)\mathrm{d}t\right)^2\right] \quad (1)$$

where T_f – the period of following the frame scan of the monitor screen with the LCS, T_a – analysis time $T_a \in [T_{a\,\min}, T_{a\,\max}]$, $T_{a\,\min}$, $T_{a\,\max}$ – lower and upper analysis time limits, k – harmonic number with information harmonic frequencies k/T_f, k = 1, 2, …, K, ($K \approx 3.3\cdot10^7$, for T_f =1/60 Hz). To calculate (1), the signal implementation is analyzed

$$x(t) = \begin{cases} n(t), & \text{when the signal is not present} \\ n(t) + s(t, \mathbf{v}_0), & \text{when the signal is present} \end{cases} \quad (2)$$

where $n(t)$ – White Gaussian noise (WGN) with one-way spectral power density N_0 and the correlation function:

$$B(t_1, t_2) = \frac{N_0}{2}\delta(t_2 - t_1) \quad (3)$$

$s(t, \mathbf{v}_0)$ – SR signal, continuous in time t, $\mathbf{v}_0$ – vector of actual values of unknown parameters of the SR signal, $\delta(x)$ – Delta function.

A compatible algorithm for detecting SR and estimating the time interval at which they do not change consists in comparing the absolute maximum of (1) with the detection threshold h, at which a decision is made to detect SR from the monitor screen when

$$\sup_{T_{a\,\min} \le T_a \le T_{a\,\max}} L(T_a) > h \quad (4)$$

and the decision that there is no SR signal – when $\sup_{T_{a\,\min} \le T_a \le T_{a\,\max}} L(T_a) \le h$.

The scheme of the asymptotically Bayesian compatible algorithm for detecting the SR signal and estimating the duration used in modern STMEI is shown in Fig. 1. It consists of K – energy storage channels k – x harmonics in quadratures, K – adders in processing channels from $T_{a\,\min}$ to $T_{a\,\max}$, maximum selection devices (MSD) and a comparison scheme with the detection threshold h.

1. Problem statement

To find out the effectiveness of modern STMEI, it is necessary to answer a simple question: at what distances from the monitor screens with the LCS, SR will be detected. It will not go into the specifics of the propagation of radio waves in the near zone and will assume that the electric and magnetic components of the SE near the STMEI are formed the same as for a wave in the far zone, that is, at distances of tens and hundreds of meters from monitor screens.

Let us find the quality indicators of signal detection by the asymptotically optimal (asymptotically Bayesian) compatible algorithm for detecting SEMR&T and estimating the duration of a static image on the monitor screen (Fig. 1) at certain distances of the STMEI from the monitor screens with LCS: probability of false alarm

$$\alpha = 1 - F_0(h, T_a/0) \quad (5)$$

and the probability of signal miss:

$$\beta = F_0(h, T_a/1) \quad (6)$$

where $F_0(x, T_a/0)$, $F_0(x, T_a/1)$ – distribution of absolute maxima (DAM) of process (2) when in the implementation $x(t)$ of the signal there is no SEMR&T and when it is present, respectively. Approaches to the analysis of the signal processing algorithm (Fig. 1) using the apparatus of one-component Markov processes is highlighted in [1–3, 5, 7], and using two-component Markov processes – in [4, 6].

Since the solution to the problem of analyzing quality indicators of STMEI will depend on a specific "picture" on the monitor screen and a specific vector of parameters $\mathbf{v}_0 = (a_{1c0}, a_{1s0}, a_{2c0}, a_{2s0}, .., a_{Kc0}, a_{Ks0})$, for any SR signal with a frame tracking period T_f, which do not change on the monitor screen over time T_{a0}, the energy of the SR signal will amount to:

$$E = \int_0^{T_{a0}} s^2(t, \mathbf{v}_0)\,\mathrm{d}t \tag{7}$$

and will manifest itself, according to (2), through the deterministic component of the random process (1):

$$\det\left[L(T_{a0}, K)\right] = \frac{4}{N_0 T_{a0}} \sum_{k=1}^{K} a_{k0}^2 \times$$
$$\times \left[\left(\int_0^{T_{a0}} \cos\left(\frac{2\pi k t}{T_f} - \phi_k \right) \cos\left(\frac{2\pi k t}{T_f} \right) \mathrm{d}t \right)^2 + \right. \tag{8}$$
$$\left. + \left(\int_0^{T_{a0}} \cos\left(\frac{2\pi k t}{T_f} - \phi_k \right) \sin\left(\frac{2\pi k t}{T_f} \right) \mathrm{d}t \right)^2 \right]$$

a_{k0}^2 – squares of amplitudes k – x harmonics, k = 1, 2, …, K which are sent to the STMEI with initial phases ϕ_k, and are associated with quadratures $a_{kc0} = a_{k0}\cos(\phi_k)$, $a_{ks0} = a_{k0}\sin(\phi_k)$, estimates of which can be obtained by processing the input implementation of the signal in the STMEI:

$$\hat{a}_{kc0} = \frac{2}{T_{a0}} \int_0^{T_{a0}} x(t) \cos\left(\frac{2\pi k t}{T_f} \right) \mathrm{d}t \tag{9a}$$

$$\hat{a}_{ks0} = \frac{2}{T_{a0}} \int_0^{T_{a0}} x(t) \sin\left(\frac{2\pi k t}{T_f} \right) \mathrm{d}t \tag{9b}$$

Estimates of (9) are more accurate than of (7) and T_{a0}/T_f is higher.

Let us simplify the problem by considering the SR signal for which $\forall k$ = 1, 2, …, K,

$$a_{kc0}^2 + a_{ks0}^2 = a_{k0}^2 = a^2 = \mathrm{const} \tag{10}$$

a^2 – SR signal strength at any k-th harmonic. Signal (10) is similar in properties to WGN, which has a constant spectral power density N_0. But unlike WGN, which will look like "snow" on a black-and-white monitor screen, this signal looks like a chaotic in terms of brightness, but static (not variable) "picture", the view of which is modeled in the MathCad environment, for the monitor of 800×768 pixels with T_f = 1/60 Hz. The generated signal was normalized to a maximum value of 255 and converted using the WRITEBMP("data.bmp") to the graphic image file shown in Fig. 2, for different values a^2.

The selected test signal obviously has maximum entropy. Therefore, if it is detected by the STMEI, any image with the same energy on the monitor screen, the leak from which is being investigated, it will be undoubtedly "intercepted" by the STMEI with indicators better than (6) for fixed values (5) (Neumann-Pearson criterion).

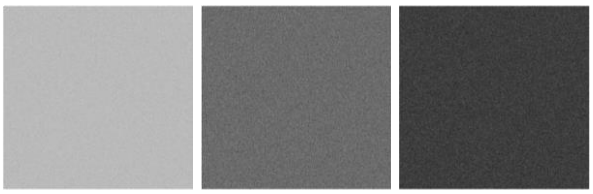

a) b) c)

Fig. 2. View of the test signal on the monitor screen: a) for $a^2 = a_1^2$, b) for $a^2 = a_2^2$, c) for $a^2 = a_3^2$, $a_1^2 < a_2^2 < a_3^2$

Taking into account (10), for $T_{a0}/T_f = T_{a0}^*$, expression (8) can be represented as follows:

$$\det\left[L(T_{a0}, K)\right] = q^2 + \frac{q^2}{16\pi^2 T_{a0}^{*2} K} \sum_{k=1}^{K} \frac{1}{k^2} \sin\left(4\pi k T_{a0}^*\right) -$$
$$- \frac{q^2}{\pi T_{a0}^* K} \sum_{k=1}^{K} \frac{1}{k} \sin(2\phi_k) \left[1 - \cos\left(4\pi k T_{a0}^*\right)\right] \tag{11}$$

which is simplified when $T_{a0} >> T_f$ ($T_{a0}^* \to \infty$) or $K \to \infty$:

$$\det\left[L(T_{a0}, K)\right] = \frac{a^2 K T_{a0}}{N_0} = q^2 K \tag{12}$$

q^2 – output signal-to-noise ratio T_a – the STMEI receiver channel (Fig. 1), if there is an SR signal from the monitor screen, to which the rating $\hat{T}_{a0}$ corresponds.

Objective: find quality indicators of signal detection using the algorithm (4): the probability of false alarm (5) and signal miss (6), depending on the energy indicators of the SR signal (7).

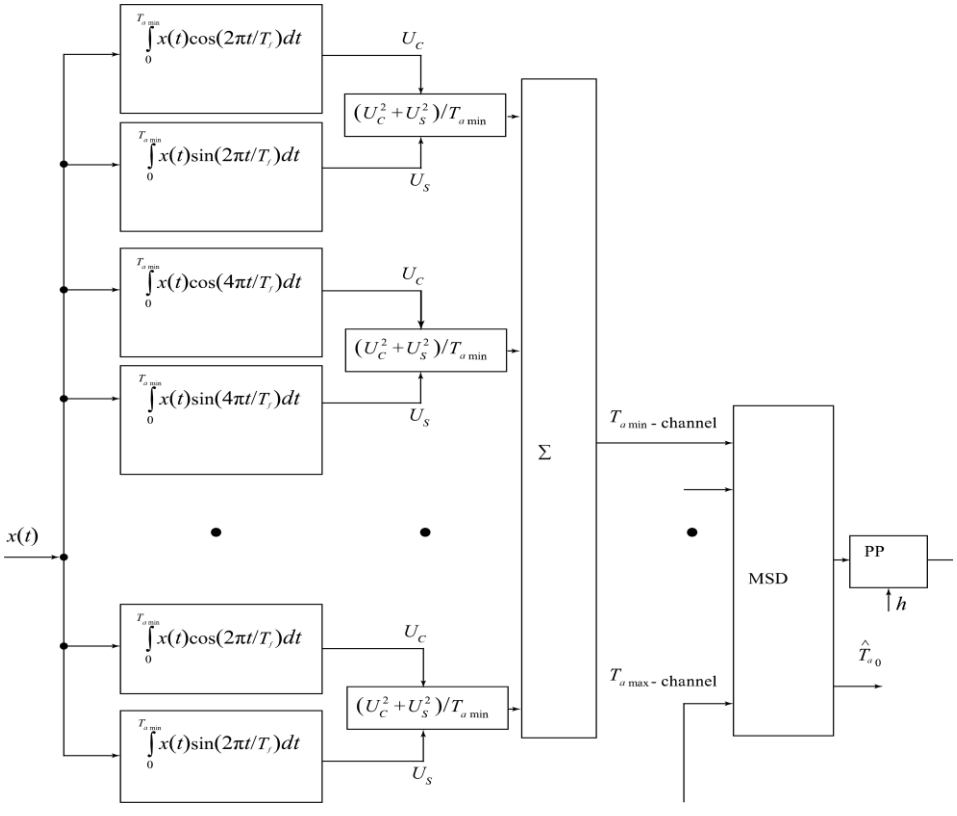

Fig. 1. Asymptotically Bayesian compatible algorithm for detecting IEMR&I and estimating the duration of a static image on a monitor screen

2. Solution of the problem of analysing the quality of side radiation detection

Whatever the signal structure $s(t,\mathbf{v}_0)$ is, its energy (7) is included in quadratures of amplitudes a_{kc} and a_{ks}, $k = 1, 2, \ldots, K$, k-th amplitude of the SR signal, and the task of analysing the quality of detection of SR signals by the STMEI is focused on the search for DAMs $F_0(x,T_a/0)$, $F_0(x,T_a/1)$ of random process (1):

$$L(T_a)=\frac{4}{N_0T_a}\xi(T_a) \tag{13}$$

in which [8]:

$$\xi(T_a)= =\sum_{k=1}^{K}\left[\left(\int_0^{T_a}x(t)\cos\left(\frac{2\pi kt}{T_f}\right)\mathrm{d}t\right)^2+\left(\int_0^{T_a}x(t)\sin\left(\frac{2\pi kt}{T_f}\right)\mathrm{d}t\right)^2\right]= \tag{14}$$

$$=\int_0^{T_a}x(t_1)\int_0^{T_a}x(t_2)\,f(t_2-t_1,K)\,\mathrm{d}t_1\mathrm{d}t_2$$

where

$$f(x,K)=\frac{\sin\left[(K+1)\pi x/T_f\right]\cos\left[K\pi x/T_f\right]}{\sin\left[\pi x/T_f\right]}-1 \tag{15}$$

When there is no SR signal at the input of the STMEI, in accordance with (2): $x(t)=n(t)$, and the random process (14) is distributed according to the law with mathematical expectation:

$$m_\xi(T_a)=\frac{N_0}{2}\int_0^{T_a}\int_0^{T_a}\delta(t_2-t_1)\,f(t_2-t_1,K)\,\mathrm{d}t_1\mathrm{d}t_2=\frac{N_0KT_a}{2} \tag{16}$$

The correlation function of process (14) can be represented as follows:

$$m_{\xi1\xi2}(T_{a1},T_{a2})=\int_0^{T_{a1}}\mathrm{d}t_1\int_0^{T_{a1}}\mathrm{d}t_2\int_0^{T_{a2}}\mathrm{d}t_3 \int_0^{T_{a2}}\langle n(t_1)n(t_2)n(t_3)n(t_4)\rangle\,f(t_2-t_1,K)\,f(t_4-t_3,K)\,\mathrm{d}t_4 \tag{17}$$

where $f(x,K)$ is set in (15), and

$$\langle n(t_1)n(t_2)n(t_3)n(t_4)\rangle= =\int_{-\infty}^{\infty}\int_{-\infty}^{\infty}\int_{-\infty}^{\infty}\int_{-\infty}^{\infty}x_1x_2x_3x_4w_4(x_1,x_2,x_3,x_4)\mathrm{d}x_1\mathrm{d}x_2\mathrm{d}x_3\mathrm{d}x_4 \tag{18}$$

$w_4(x_1,x_2,x_3,x_4)$ – four-dimensional probability density of a Gaussian stationary process $n(t)$ at points in time t_1, t_2, t_3, t_4, which, taking into account (3), is represented by the expression (19):

$$w_4(x_1,x_2,x_3,x_4)=\frac{\sigma^2}{4\pi^2\sqrt{\left(\sigma^4-N_0^2\delta^2(t_2-t_1)/4\right)\left(\sigma^4-N_0^2\delta^2(t_3-t_2)/4\right)\left(\sigma^4-N_0^2\delta^2(t_4-t_3)/4\right)}}\times$$
$$\times\exp\left[-\left(\frac{N_0^2\delta^2(t_2-t_1)}{8\sigma^2\left(\sigma^4-N_0^2\delta^2(t_2-t_1)/4\right)}+\frac{1}{2\sigma^2}\right)x_1^2-\frac{\sigma^2}{2\left(\sigma^4-N_0^2\delta^2(t_4-t_3)/4\right)}x_4^2\right]\times$$
$$\times\exp\left[-\left(\frac{N_0^2\delta^2(t_3-t_2)}{8\sigma^2\left(\sigma^4-N_0^2\delta^2(t_3-t_2)/4\right)}+\frac{\sigma^2}{2\left(\sigma^4-N_0^2\delta^2(t_2-t_1)/4\right)}\right)x_2^2\right]\times$$
$$\times\exp\left[-\left(\frac{N_0^2\delta^2(t_4-t_3)}{8\sigma^2\left(\sigma^4-N_0^2\delta^2(t_4-t_3)/4\right)}+\frac{\sigma^2}{2\left(\sigma^4-N_0^2\delta^2(t_3-t_2)/4\right)}\right)x_3^2\right]\times \tag{19}$$
$$\times\exp\left[\frac{N_0\delta(t_2-t_1)x_1x_2}{2\left(\sigma^4-N_0^2\delta^2(t_2-t_1)/4\right)}+\frac{N_0\delta(t_3-t_2)x_2x_3}{2\left(\sigma^4-N_0^2\delta^2(t_3-t_2)/4\right)}+\frac{N_0\delta(t_4-t_3)x_3x_4}{2\left(\sigma^4-N_0^2\delta^2(t_4-t_3)/4\right)}\right]$$

A substitution of (19) into (18) and integrating it by $\mathrm{d}x_4$, $\mathrm{d}x_2$, $\mathrm{d}x_1$, $\mathrm{d}x_3$ leads to the expression:

$$\langle n(t_1)n(t_2)n(t_3)n(t_4)\rangle= =\frac{N_0^4\delta(t_4-t_3)\delta^2(t_3-t_2)\delta(t_2-t_1)}{4\sigma^4}+ +\frac{N_0^2\delta(t_4-t_3)\delta(t_2-t_1)}{2} \tag{20}$$

while a substitution of (20) to (17) and integrating it by $\mathrm{d}t_4$, $\mathrm{d}t_1$, $\mathrm{d}t_2$, $\mathrm{d}t_3$ – to the expression:

$$B_\xi(T_{a1},T_{a2})= =\langle\xi(T_{a1})\xi(T_{a2})\rangle=\frac{N_0^2K^2T_{a1}T_{a2}}{2} \tag{21}$$

In addition, taking into account (20), we can find the correlation function for $k \neq l$ of spectral components of SR:

$$B_{k,l}(T_a)= =\int_0^{T_a}\mathrm{d}t_1\int_0^{T_a}\mathrm{d}t_2\int_0^{T_a}\mathrm{d}t_3\int_0^{T_a}\langle n(t_1)n(t_2)n(t_3)n(t_4)\rangle\times \times\cos\left[\frac{2\pi k(t_2-t_1)}{T_f}\right]\cos\left[\frac{2\pi l(t_4-t_3)}{T_f}\right]\mathrm{d}t_4=\frac{N_0^2T_a^2}{2}, \quad \forall k,l=1,2,..,K$$

which amounts to (21) when the sum of the series in (14) consists of only one term $K = 1$, for $T_{a1}=T_{a2}=T_a$.

This means that all random spectral components of the SR signal are correlated with each other with the unit correlation coefficient, and since $K \neq \infty$, the distribution of the sum of the spectral components in (14) is not normalized, and the variance of the random variable $L(T_a)=Kn_0^2$ (n_0 – normally distributed random variable with zero mean and unit variance) – amounts to $2K^2$. This variance has the square of a centered Gaussian random variable with the variance K. Therefore, the distribution of the random variable (13), when there is no SR, is represented as follows [8, p. 221]:

$$F(h,T_a/0)=2F\left(\sqrt{h^*}\right)-1 \tag{22}$$

$h^*=\sqrt{h/K}$ – given detection threshold,
$F(x)$ – integral normal distribution function.

Therefore, if there is no SR signal at the input of the STMEI, the process (13) is distributed according to the law (22), while the correlation function of the Gaussian process forming (13) will be equal to:

$$B_L\left(T_{a1},T_{a2}\right)=\frac{KT_{a1}T_{a2}}{T_a^2} \tag{23}$$

and the desired probability of false alarm (5) can be calculated in accordance with [8, p. 170]:

$$\alpha=1-F\left(h,T_{a1}/0\right)\exp\left(-\int_{T_{a1}}^{T_{a2}}\frac{\pi\left(h,t/0\right)}{F\left(h,t/0\right)}\,\mathrm{d}t\right) \tag{24}$$

where $F\left(h,t/0\right)$ is set (22),

$$\pi\left(h,t/0\right)=\int_0^\infty y w_2\left(h,y,t/0\right)\,\mathrm{d}y= \\ =\sqrt{\frac{2h}{\pi}}\frac{B_{LL'}}{\sigma_L^3}\exp\left[-\frac{h}{2\sigma_L^2}\right] \tag{25}$$

$w_2\left(h,y,T_a/0\right)$ – two-dimensional probability density of the process distribution $L\left(T_a\right)$ and its derivative $L'\left(T_a\right)$ at identical points in time, having the parameters:

$$\sigma_L^2=\sigma_L^2\left(T_a\right)=B_L\left(T_a,T_a\right)=K; \\ B_{LL'}=B_{LL'}\left(T_a\right)=\left.\frac{\partial B_\xi\left(T_{a1},T_{a2}\right)}{\partial T_{a2}}\right|_{T_{a1}=T_{a2}=T_a}=\frac{K}{T_a}; \\ \sigma_{L'}^2=\sigma_{L'}^2\left(T_a\right)=\left.\frac{\partial^2 B_L\left(T_{a1},T_{a2}\right)}{\partial T_{a1}\partial T_{a2}}\right|_{T_{a1}=T_{a2}=T_a}=\frac{K}{T_a^2} \tag{26}$$

where $B_L\left(T_{a1},T_{a2}\right)$ – is defined (23), σ_L^2 – variance of the centered Gaussian process, $\sigma_{L'}^2$ – variance of the derivative of the centered Gaussian process; $B_{LL'}$ – mutual correlation function of the centered Gaussian process and its derivative at identical points in time.

Integrating the two-dimensional probability density in expression (25), taking into account (26), allows us to present the dependence of the probability of false alarm (24) on the, represented as follows:

$$\alpha=1-\left(2F\left(\sqrt{h^*}\right)-1\right)\cdot\left(\frac{T_{a0\max}}{T_{a0\min}}\right)^{-\sqrt{\frac{2h^*}{\pi}}\frac{\exp\left(-\frac{h^*}{2}\right)}{\left(2F\left(\sqrt{h^*}\right)-1\right)}} \tag{27}$$

Dependence of the probability of false alarm (27) on the given detection threshold of the STMEI receiver, for $T_{a0\max}/T_{a0\min}$ = 1; 2; 10, is shown in Fig. 3. As we can see, a fixed false alarm is achieved at higher h^*, for longer intervals $T_{a0\max}/T_{a0\min}$ in the uncertainty of values T_{a0}, $T_{a0\min}\le T_{a0}\le T_{a0\max}$.

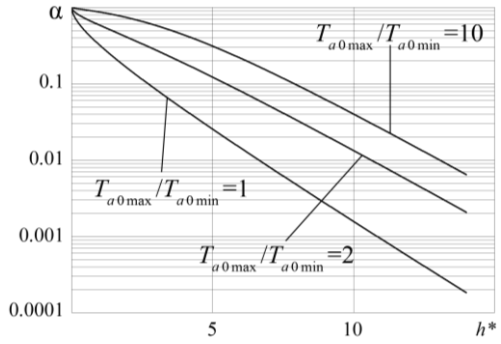

Fig. 3. Dependence of the probability of false alarm on the given detection threshold of the receiver of a specialized technical means of enemy intelligence

According to the Neumann-Pearson criterion, fixing the false alarm level (27) makes it possible to find the given detection threshold h^*, and calculate the probability of signal miss (6) when there is an SR signal at the input of the STMEI receiver. Random variable $L\left(T_a\right)$, taking into account (12), is the square of a Gaussian random variable with variance $\sigma_L^2=K$ and mathematical expectations $q\sqrt{K}$, which is distributed according to the law:

$$F\left(h,T_a/1\right)=F\left(\sqrt{h^*}-q\right)+F\left(\sqrt{h^*}+q\right)-1 \tag{28}$$

If after the time of the SR signal T_{a0} the rest of the time $T_{a0}\le T_a<T_{a0\max}$ there was no SR signal, a random variable $L\left(T_a\right)$ for $T_{a0\min}\le T_a<T_{a0}$ can be considered a non-stationary Gaussian process with mathematical expectation $q\sqrt{K}$, for $T_{a0}\le T_a<T_{a0\max}$ – with zero mathematical expectation, and the probability of signal miss (6) is calculated according to the expression

$$\beta=F\left(h,T_{a1}/1\right)\exp\left(-\int_{T_{a1}}^{T_{a2}}\frac{\pi\left(h,t/1\right)}{F\left(h,t/1\right)}\,\mathrm{d}t\right) \tag{29}$$

where $F\left(h,t/1\right)$ is set (28),

$$\pi\left(h,t/1\right)=\int_0^\infty y w_2\left(h,y,t/1\right)\,\mathrm{d}y= \\ =\frac{B_{LL'}\left(\sqrt{h}-q\sqrt{K}\right)\cdot\mathbf{1}\left(\sqrt{h}-q\sqrt{K}\right)}{2\sqrt{2\pi h}\sigma_L^2}\times\exp\left[-\frac{\left(\sqrt{h}-q\sqrt{K}\right)^2}{2\sigma_L^2}\right]+ \\ +\frac{B_{LL'}\left(\sqrt{h}+q\sqrt{K}\right)}{\sqrt{2\pi}\sigma_L^3}\exp\left[-\frac{\left(\sqrt{h}+q\sqrt{K}\right)^2}{2\sigma_L^2}\right] \tag{30}$$

$\mathbf{1}(x)$ – single function.

At the same time, for any T_{a0} process parameters $L\left(T_a\right)$ as before, will be calculated taking into account (26), and the desired probability of signal miss (29), taking into account (30), will be equal to:

$$\beta=\left[F\left(\sqrt{h^*}-q\right)+F\left(\sqrt{h^*}+q\right)-1\right]\times \\ \times\left(\frac{T_{a0}}{T_{a0\min}}\right)^{-\frac{\left(\sqrt{h^*}-q\right)\exp\left(-\frac{\left(\sqrt{h^*}-q\right)^2}{2}\right)\cdot\mathbf{1}\left(\sqrt{h^*}-q\right)+\left(\sqrt{h^*}+q\right)\exp\left(-\frac{\left(\sqrt{h^*}+q\right)^2}{2}\right)}{\sqrt{2\pi}\left[F\left(\sqrt{h^*}-q\right)+F\left(\sqrt{h^*}+q\right)-1\right]}}\times \\ \times\left(\frac{T_{a0\max}}{T_{a0}}\right)^{-\sqrt{\frac{2h^*}{\pi}}\frac{\exp\left(-\frac{h^*}{2}\right)}{\left(2F\left(\sqrt{h^*}\right)-1\right)}} \tag{31}$$

in which h^* is found according to (27), for a fixed α, while q – defined by (12).

In Fig. 4 the dependences of the probabilities of correct signal detection $1-\beta$ from the parameter q, for α = 0.01, $T_{a0\max}/T_{a0\min}$ = 1; 2; 10 and $T_{a0}/T_{a0\min}$ = 1. As expected, with increasing uncertainty $T_{a0\max}/T_{a0\min}$ the detection curves are dislocated to the right.

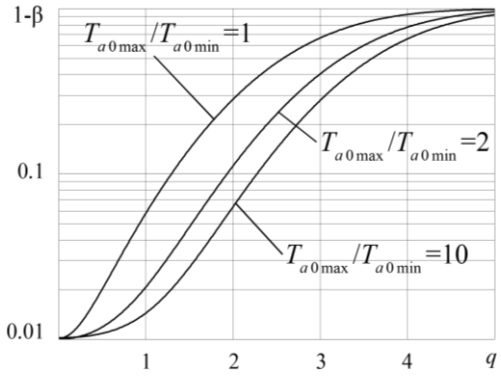

Fig. 4. Probability of correct detection of information leakage signals from the monitor screen, for $T_{a0}/T_{a0\min}=1$

3. Modeling in MathCAD and Excel environments

Let us investigate the correctness of the calculation using expressions (27) and (31). For this purpose, we will simulate the process of exceeding the detection threshold h in the tool (Fig. 1), when the input of the STMEI, in accordance with (2), receives the implementation of WGN or the sum of SR with the characteristics of (10) and WGN. At the same time, WGN is given close to δ – correlated normally distributed array n_i, i = 1, 2, …, N, with zero mean and variance σ^2, N – array volume. The array with these characteristics is generated in the Mathcad software environment, and its further processing in the Excel software environment allows to conveniently controlling all the statistical characteristics of intermediate digital arrays and making sure that the simulation results obtained are reliable.

For the statistical validity of the estimates generated when creating the model, it is necessary to operate n independent tests on arrays with N/n elements, while to estimate, for example, the probability of a false alarm $\alpha = 0.01$, it is necessary to have more than $n = 100$ tests. If $N = 15000$ arrays that can be used for statistical processing will have volumes less than 150 samples. That is, during the simulation of the process at time intervals $t \in [0, T_a]$ integrals in expression (14) are replaced by sums:

$$\Delta t \sum_{i=1}^{\mathrm{ceil}(T_a/\Delta t)} n_i \cos\left(\frac{2\pi k \Delta t i}{T_f}\right),\ \Delta t \sum_{i=1}^{\mathrm{ceil}(T_a/\Delta t)} n_i \sin\left(\frac{2\pi k \Delta t i}{T_f}\right)$$

where $\mathrm{ceil}(x)$ – the whole part of x, Δt – time interval for sampling the process.

In Fig. 5 solid lines represent the dependences of probabilities of a false alarm on the detection threshold, for small K = 20; 30; 50 and $T_{a0\max}/T_{a0\min}$ = 1, calculated according to (27). The triangles in the figure illustrate the results of modelling the process of false signal detection for If N = 15000 and n = 1000 ($T_a = 15\Delta t$).

As you can see, the results of calculations are quite accurately confirmed by practice, especially for small K. Increasing discrepancies between theory and practice, with increasing K, is associated with an increase in variance $\sigma_L^2 = K$ and the need to increase the number of independent software tests to create a more adequate model of false signal detection.

In the case when SR is observed by STMEI, for $T_{a0\max} = T_{a0\min} = T_{a0}$ simulation of the correct detection process using a noise array with N = 15000 samples is possible only for small ratios T_{a0}/T_f, since $T_{a0} = 15\Delta t$. In this case, the interval Δt, in fact, determines the time when one pixel of information is emitted from the monitor screen. Therefore, even without taking into account the time for transmitting string synchronization pulses [10] for a monitor with a scan of 800×768 pixels $T_f > 614400\Delta t$, while $T_{a0}/T_f < 2.4\cdot10^{-5}$.

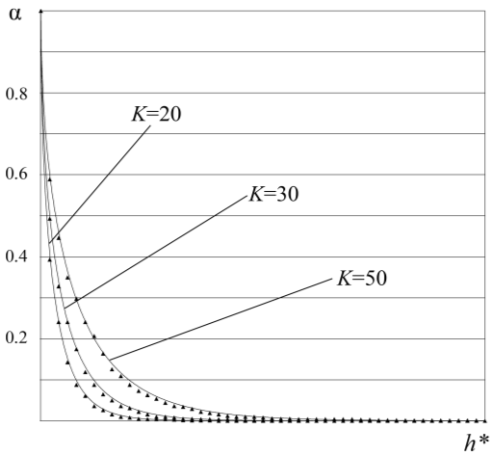

Fig. 5. Calculated and modeled dependences of probabilities of a false alarm on the reduced detection threshold of the STMEI receiver

In Fig. 6–8 solid lines illustrate the dependences calculated using (31) of the probabilities of correct detection of the SR signal $1-\beta$ from the given threshold h^*, for small K = 20; 30; 50, $T_{a0\max}/T_{a0\min}$ =1, and q = 1 – Fig. 6, q = 2 – Fig. 7, q = 3 – Fig. 8. For comparison, triangles indicate the results of modeling the process of passing the SR signal. As you can see, the results of calculations according to (28) are almost perfectly confirmed by modeling the process in the Mathcad and Excel software environment, at least for $T_{a0\max} = T_{a0\min} = T_{a0}$.

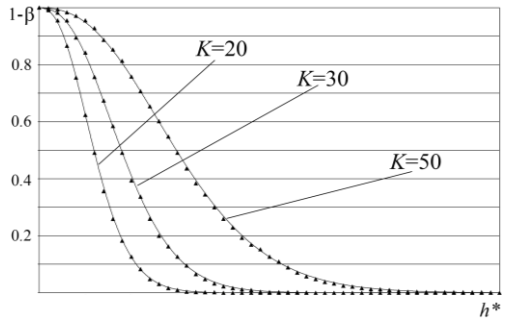

Fig. 6. Calculated and modeled the dependences of the probabilities of correct detection of SR on the given detection threshold of the STMEI receiver, for q = 1

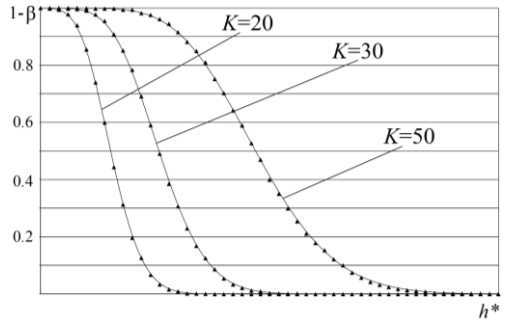

Fig. 7. Calculated and modeled the dependences of the probabilities of correct detection of SR on the given detection threshold of the STMEI receiver, for q = 2

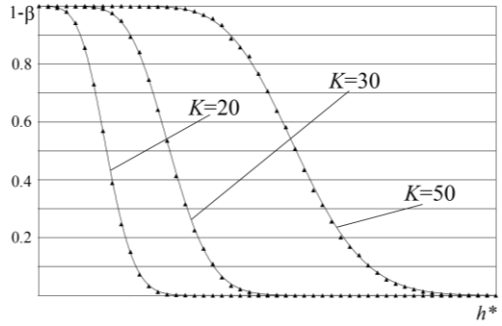

Fig. 8. Calculated and modeled the dependences of the probabilities of correct detection of SR on the given detection threshold of the STMEI receiver, for q = 3

In order to use the same software to create an adequate model for studying the correct detection of the SR signal, for $T_{a0\max} / T_f = T^*_{a0\max}$, it is necessary to increase the noise signal array to $N = 6.25 \cdot 10^8 T^*_{a0\max}$, which is unrealistic neither in the Mathcad environment nor in the Excel environment. In addition, for processing $K \approx 3.3 \cdot 10^7$, for T_f = 1/60 Hz (and not as it was investigated for $K = 50$) it is necessary to multiply $6.6 \cdot 10^5$ times the size of the substitution tables in the Excel software environment, which is also impossible to do. In addition, the study of expression (25) for $T_{a0\max} \neq T_{a0\min}$ will require approximately $T_{a0\max} / T_{a0\min}$ times larger amounts of calculations, which is possible only with the use of professional programs for processing information arrays in C++ or C sharp software environments.

Conclusions

1. The expressions found in this paper for calculating the probability of false alarm and signal miss of information leakage from monitor screens for a specialised enemy reconnaissance vehicle are confirmed by modelling the processes of false and correct detection of side radiation signals in the Mathcad and Excel software environments, at least when there is no a priori uncertainty about the time of change of the static image on the monitor screen.
2. Finally, the reliability of the obtained expressions for calculating the quality indicators of detecting signals of side radiation from monitor screens should be confirmed by additional modelling of the process of detecting information leakage by processing significant data sets in the C++ or C sharp software environments.

References

[1] Adler R. J.: Random field and geometry. Springer, New York 2007.
[2] Adler R. J.: Random field and their geometry. Springer, New York 2003.
[3] Behl D., Handa S., Arora A.: A bug Mining tool to identify and analyze security bugs using Naive Bayes and TF-IDF. International Conference on Reliability Optimization and Information Technology – ICROIT, IEEE 2014, 294–299.
[4] Chmielowski L., Kucharzak M.: Impact of Software Bug Report Preprocessing and Vectorization on Bug Assignment Accuracy. Progress in Image Processing, Pattern Recognition and Communication Systems. Springer, Cham 2022.
[5] Gnedenko B. V.: Sur la distribution limite du terme maximum d'une serie aleatore. Annals of Mathematics. 44(3), 1943, 423–453.
[6] Leadbetter V. R.: Extreme value theory for continuous parameter stationary processes. Technical rept. ADA083802, 1980-03-01.
[7] Leadbetter V. R., Lindgren G., Rootzen H.: Extreme and Related Properties of Random Sequences and Processes. Springer, New York 1983.
[8] Marple S. L.: Digital spectral analysis: with application. Prentice Hall, New Jersey 1987.
[9] Yevgrafov D. V., Yaremchuk Y. Y.: Asymptotically optimal algorithm for processing side radiation signals from monitor screens on liquid crystal structures. Informatyka, Automatyka, Pomiary w Gospodarce i Ochronie Środowiska – IAPGOS 13(4), 2023, 99–102.
[10] Yevgrafov D. V., Yaremchuk Y. Y.: Calculated spectra of information leakage signals from monitor screens with liquid crystal structures. Registration, storage and processing of data 23(2), Kyiv 2021, 3–12.

Ph.D. Dmytro V. Yevgrafov
e-mail: yevg.dmytro@gmail.com

The Ph.D. (Engineering), and the senior researcher. He is the author of more than 50 scientific academic papers, including 2 monographs, 45 articles in scientific specialized publications, 4 training manuals, materials and abstracts of reports at academic conferences.
The author's scientific interests are in statistical radio engineering, radio electronic intelligence and physical protection of information.

https://orcid.org/0000-0001-9651-1558

D.Sc. Eng. Yurii Ye. Yaremchuk
e-mail: yurevyar@vntu.edu.ua

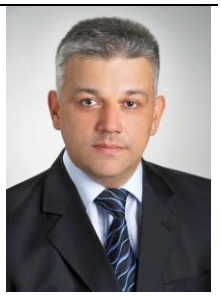

The Doctor of Science in Engineering, and the professor. He is the author of more than 300 publications, including 2 monographs, 140 articles in scientific specialized publications, 20 textbooks and training manuals, 20 utility model patents and 25 certificates of copyright registration for work.
The author's scientific interests are in cryptographic and steganographic protection of information, technical protection of information and security of information systems.

https://orcid.org/0000-0002-6303-7703